



Published in final edited form as:

J Hepatol. 2018 April ; 68(4): 744–753. doi:10.1016/j.jhep.2017.12.016.

Adult hepatocytes direct liver organogenesis through non-parenchymal cell recruitment in the kidney

Rie Utoh^{1,2}, Junji Komori^{3,4}, Hiroyuki Kuge⁵, Kohei Tatsumi^{1,6}, Masumi Yamada², Shinji Hirohashi⁷, Masahiro Tsutsumi⁸, Toshihiro Amanuma⁹, Akira Yoshioka¹⁰, Yoshiyuki Nakajima⁵, Kenjiro Wake¹¹, Teruo Okano¹, Eric Lagasse³, and Kazuo Ohashi^{1,5,12,*}

¹Institute of Advanced Biomedical Engineering and Science, Tokyo Women's Medical University, Tokyo, Japan

²Department of Applied Chemistry and Biotechnology, Graduate School of Engineering, Chiba University, Chiba, Japan

³Department of Pathology, McGowan Institute for Regenerative Medicine, University of Pittsburgh School of Medicine, Pittsburgh, PA, USA

⁴Department of Surgery, Takamatsu Red Cross Hospital, Kagawa, Japan

⁵Department of Surgery, Nara Medical University, Nara, Japan

⁶Department of Physiology and Regenerative Medicine, Kindai University Faculty of Medicine, Osaka, Japan

⁷Department of Radiology, Nara Medical University, Nara, Japan

⁸Department of Pathology, Saiseikai Chuwa Hospital, Nara, Japan

⁹Research Center, Nihon Nohyaku Co., Ltd., Osaka, Japan

¹⁰Nara Medical University, Nara, Japan

¹¹Liver Research Unit, Minophagen Pharmaceutical Co., Ltd., Tokyo, Japan

*Corresponding Author: Kazuo Ohashi, M.D., Ph.D., Laboratory of Drug Development and Science, Graduate School of Pharmaceutical Sciences, Osaka University, 1-6 Yamadaoka, Suita, Osaka 565-0871, Japan, ohashikazuo@hotmail.com, Tel: +81-6-6879-8144.

Publisher's Disclaimer: This is a PDF file of an unedited manuscript that has been accepted for publication. As a service to our customers we are providing this early version of the manuscript. The manuscript will undergo copyediting, typesetting, and review of the resulting proof before it is published in its final citable form. Please note that during the production process errors may be discovered which could affect the content, and all legal disclaimers that apply to the journal pertain.

Conflict of interest: Drs. Amanuma and Wake are employees of Nihon Nohyaku Co., Ltd. (Osaka, Japan) and Minophagen Pharmaceutical Co., Ltd. (Tokyo, Japan), respectively, unrelated to the submitted work. Dr. Okano is a chairman and a scientific advisory board of CellSeed, Inc., outside the submitted work. Dr. Ohashi received a research grant from Bayer, during the conduct of the study. No other relationships or activities that could appear to have influenced the submitted work are reported. Please refer to the accompanying ICMJE disclosure forms for further details.

Authors contributions:

R.U. and K.O. designed experimental strategy, performed experiments, and analyzed the data assisted by H.K. and K.T. J.K. performed in vivo experiments using *Fah*^{-/-} mice and the data analysis. M.T. performed histology and data analysis. S.H. performed MRI analysis. T.A. and K.W. performed observation with transmission electron microscope and the data analysis. R.U., J.K., M.Y. and K.O. drafted the manuscript. M.Y., A.Y., Y.N., K.W., E.L., and T.O. interpreted the data and supervised the study.

Transcript profiling: Microarray data are deposited in GEO (GEO accession: GSE99141).

¹²Laboratory of Drug Development and Science, Graduate School of Pharmaceutical Sciences, Osaka University, Osaka, Japan

Abstract

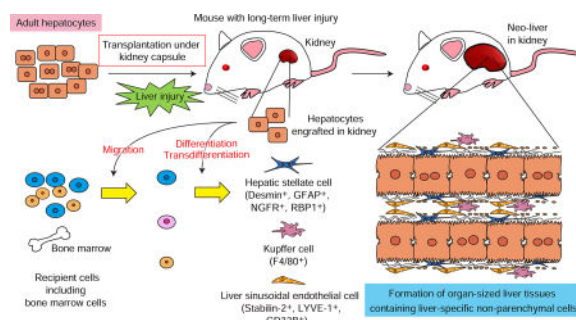
Background & Aims—Since the first account of the myth of Prometheus, the amazing regenerative capacity of the liver has fascinated researchers due to its enormous medical potential. Liver regeneration is promoted by multiple types of liver cells, including hepatocytes and liver non-parenchymal cells (NPCs), through the complex intercellular signaling. However, the liver organogenetic mechanism, especially the role of adult hepatocytes at ectopic sites, remains unknown. In this study, we demonstrate that hepatocytes alone spurred liver organogenesis to form an organ-sized complex 3D liver that exhibited native liver architecture and functions in the kidneys of mice.

Methods—Isolated hepatocytes were transplanted under the kidney capsule of monocrotaline (MCT) and partial hepatectomy (PHx)-treated mice. To determine the origin of NPCs in neo-livers, hepatocytes were transplanted into MCT/PHx-treated green fluorescent protein (GFP) transgenic mice or wild-type mice transplanted with bone marrow (BM) cells isolated from GFP mice.

Results—Hepatocytes engrafted at the subrenal space of mice underwent continuous growth in response to a chronic hepatic injury in the native liver. More than 1.5 yrs later, whole organ-sized liver tissues having a greater mass than those of the injured native liver had formed. Most remarkably, we revealed that at least three types of NPCs with similar phenotypic features to the liver NPCs were recruited from the host tissues including BM. The neo-livers in the kidney exhibited liver-specific functions and architectures, including sinusoidal vascular systems, zonal heterogeneity, and emergence of bile duct cells. Furthermore, the neo-livers successfully rescued the mice with lethal liver injury.

Conclusion—Our data clearly showed that adult hepatocytes play a leading role as organizer cells in liver organogenesis at ectopic sites via NPC recruitment.

Graphical abstract



Keywords

Ectopic site; Neo-liver; Non-parenchymal cells; Hepatocytes; Liver injury; Organogenesis

Introduction

The liver is a complex organ that plays central roles in metabolism, protein/enzyme synthesis, and blood detoxification, and is the sole solid organ in the body that possesses high regenerative capability. Adult hepatocytes have great growth potential in vivo, similar to that of adult stem cells.¹ Following the loss of liver mass, compensatory regenerative responses are accelerated until the original liver mass is restored, and this process is promoted by cytokines, growth factors, and hormones secreted from hepatocytes and liver non-parenchymal cells (NPCs), and other organs via complex interactions.^{2,3} Transplantation of a small number of hepatocytes to the liver has been shown to lead to complete or near-complete repopulation of the diseased livers of animal models such as urokinase-type plasminogen activator (uPA)-transgenic (Tg) or fumarylacetoacetate hydrolase (*Fah*)-deficient mice,⁴⁻⁶ ultimately reversing the lethality of these mouse models.

Previous studies have reported that hepatocytes transplanted at ectopic sites such as the spleen, subrenal capsule, and lymph nodes proliferated and formed liver-like tissues in animal models with liver injury.⁷⁻⁹ The propagated hepatocytes at these sites were functional and had therapeutic potency for liver diseases. Approaches using engineered tissues from isolated hepatocytes have also been empirically investigated to create *de novo* functional liver systems.¹⁰ For example, hepatocyte sheets prepared using temperature-responsive dishes, have been successfully transplanted into subcutaneous sites, following prevascularization by basic fibroblast growth factor (bFGF)-releasing devices to promote the sheet engraftment and the formation of liver-like tissues.¹¹ These studies clearly verified the usefulness and potential of the *de novo* creation of ectopic liver systems. However, the mechanism of liver organogenesis at ectopic sites only from adult hepatocytes remains largely unknown. Until now, morphology and function of the generated liver-like tissues at ectopic sites, including the emergence of NPCs, have not been investigated in detail.

In this study, we designed experiments to investigate whether adult hepatocytes transplanted at an ectopic site could continuously proliferate and form an organ-sized neo-liver, in response to a chronic hepatocellular injury of the native liver in mice induced by monocrotaline (MCT) treatment and partial hepatectomy (PHx).¹² We selected the subrenal capsule space as the transplantation site of hepatocytes, because (i) it allows hepatocytes to be engrafted to the host tissue without the need for prevascularization, (ii) there is a sufficient space for hepatocyte growth, and (iii) the formed liver-like tissue is separated from and not mixed with the kidney parenchyma. We discovered that adult hepatocytes are able to induce liver organogenesis through self-duplication and NPC recruitment from recipient tissues including bone marrow (BM). The engrafted hepatocytes in the subrenal capsule space finally formed an organ-sized, complex neo-liver with specific architectural characteristics of the native liver, including the emergence of NPCs with similar phenotypic features to the liver NPCs [hepatic stellate cells (HSCs), Kupffer cells (KCs), and liver sinusoidal endothelial cells (LSECs)], proper arrangement of parenchymal/NPCs, formation of liver-specific vascular networks and liver zonation, and distribution of extracellular matrix (ECM) components, in response to the chronic hepatocyte injury of the native liver. Our long-term observations thus revealed for the first time the “superior” potency of adult

hepatocytes in not only hepatocyte growth but also organogenesis of a functional liver system that exhibited the native liver-specific architecture.

Materials and methods

Animals

All animal studies were referred to the ARRIVE guidelines and were followed the institutional guidelines outlined by the Institutional Animal Care and Use Committees at Nara Medical University, Tokyo Women's Medical University, and University of Pittsburgh. Human α 1-antitrypsin (hA1AT) promoter/*hA1AT*-Tg mice (FVB/N-Tg(*hA1AT*); 8–20 wks old; kindly provided by Dr. G. L. Bumgardner), C57BL/6NCrSlc mice (7–9 wks old; Japan SLC, Shizuoka, Japan), and C57BL/6-Tg(*UBC-GFP*)30Scha/J mice (5–8 wks old; the Jackson Laboratory, Bar Harbor, ME) were used to obtain hepatocytes for transplantation. FVB/N mice (7–9 wks old; CLEA Japan, Tokyo, Japan), C57BL/6-Tg(*CAG-EGFP*) mice (7–9 wks old; Japan SLC), and *Fah*^{-/-} mice backcrossed into the C57BL/6 mouse background (12 wks old; 129sv; kindly provided by Dr. M. Grompe) were used as the recipients. Mice were housed in cages within a temperature and humidity controlled room (22–24°C, 55 ± 10% humidity) with a 12 h light/12 h dark cycle. All mice were fed a normal chow diet with *ad libitum* access to water and food.

For further details, please refer to the Supplementary Material and CTAT table.

Results

Formation of an organ-sized ectopic neo-liver under the kidney capsule

To investigate the long-term proliferation and neo-liver formation potential of hepatocytes, we transplanted 1×10^6 hepatocytes isolated from human α 1-antitrypsin (*hA1AT*)-Tg mice under the kidney capsule of wild-type mice treated with MCT, which strongly inhibits hepatocyte proliferation. One week later, the recipient mice were subjected to a 70% PHx to induce chronic hepatocellular injury. The functional volumes of the donor hepatocytes were monitored by periodically measuring the serum hA1AT levels (Fig. 1A). The hA1AT levels in the MCT/PHx mice progressively increased over the 300-day period, which correlated with the gradual thickening of the hA1AT⁺/albumin⁺ hepatic tissue under the kidney capsule (Fig. 1B, C). In marked contrast, the ectopically transplanted hepatocytes failed to expand beyond a one- to two-hepatocyte (~30 μ m)-thick tissue in mice whose livers were intact (Fig. 1C). The proliferative indices of both bromodeoxyuridine (BrdU) and cyclin D in the transplanted hepatocytes were significantly higher in the MCT/PHx mice than in the non-injured mice (Fig. S1A, B). The progressive growth of the ectopic neo-liver was further analyzed in some of the recipient mice at time points beyond 1.5 yrs. In the mice with MCT/PHx-induced chronic liver injury, the host livers were atrophied, whereas the neo-livers were massively enlarged under the kidney capsule (Fig. 2A–C; n = 2 mice). In one recipient mouse, the total mass of the left kidney, including the neo-liver, was 1.68 g at 2.4 yrs, whereas the mass of the right kidney, which did not receive a transplant, was 0.25 g. The total masses of the atrophied host liver (0.43 g) and the neo-liver (1.43 g = 1.68 - 0.25 g) in the MCT/PHx-treated mice were nearly equal to the mass of the native liver (1.8 g) from an

age-matched normal mouse. In the other recipient mouse, the masses of the injured liver, right kidney, and left kidney were 0.625 g, 0.31 g, and 1.59 g, respectively, at 1.5 yrs. Pathological findings associated with neoplasm or sarcoma formation were not observed in the neo-livers (Fig. 2D, E). Formation of such organ-sized neo-liver is an unprecedented finding, and these data indicate that hepatocytes implanted at an ectopic site are capable of continuously proliferating over a period of 1 yr in response to a chronic injury of the native liver.

Emergence of NPCs and bile duct cells in the neo-liver

Subsequently, we histologically observed the NPC components and the neo-liver structure during the organogenesis of the neo-livers (Fig. 3A). The liver consists of parenchymal cells and at least three types of NPCs, i.e., LSECs, HSCs, and KCs. In the neo-livers, desmin⁺ (a marker for HSCs¹³) cells were initially detected on day 30, and F4/80⁺ and stabilin-2⁺ (markers for KCs and LSECs, respectively^{14,15}) cells were detected on or after day 60. Notably, F4/80⁺ and stabilin-2⁺ cells were not observed in the kidney parenchyma. At day 150, the densities of these three types of NPCs were comparable to those in the normal liver. Desmin⁺ cells were also positive for other markers for HSCs [glial fibrillary acidic protein (GFAP), nerve growth factor receptor (NGFR, also known as p75NTR), retinol binding protein 1 (RBP1)].¹³ These desmin⁺ cells were found to be negative for α -smooth muscle actin, a marker for activated HSCs (Fig. S2). The endothelial cells lining along the sinusoids also expressed LYVE-1 (a marker for LSECs located in zone 2), and CD32B (a marker for LSECs) in the neo-liver (Fig. S3A).¹⁶ At day 180, vascular networks in the *de novo* engineered neo-livers were visualized following the infusion of fluorescein isothiocyanate (FITC)-conjugated *Lycopersicon esculentum* (tomato) lectin, a highly selective marker for vascular endothelial cells (ECs)¹⁷ (Fig. 3B). Cord-like cell arrangements were separated by sinusoid-like vascular spaces in which a single layer of hepatocytes was surrounded by lectin-bound ECs. The vascular spaces were also positive for type IV collagen, which is a characteristic ECM component deposited in the subsinusoidal space (Fig. S3B). The ultrastructural examination of the neo-livers by transmission electron microscopy on day 150 clarified that the neo-livers formed a perivascular space between hepatocytes and a layer of ECs, and HSC-like cells resided in this subsinusoidal space (Fig. 3C). Bile canaliculi, sealed by the tight junctions, were formed between three neighboring hepatocytes (Fig. 3D). Lipid vesicles were detected in the canalicular lumen, indicating bile acid secretion from hepatocytes.¹⁸ LSECs are highly specialized ECs that exhibit fenestrations (transcellular pores).¹⁶ These characteristic fenestrations were also abundant in the ECs (Fig. 3E, S3C). These observations revealed the extremely high similarity in terms of structure and cell composition between the neo-liver and the non-injured native liver.

To determine whether the NPCs populating the neo-livers (termed neo-liver NPCs) originated from the donor cells or recipient tissues, we generated neo-livers in *GFP-Tg* mice using GFP⁺ hepatocytes and performed an immunofluorescence analysis on days 70–120 (Fig. 3F). The cytoplasmic GFP was clearly co-localized with all examined markers, i.e., desmin, F4/80, and LYVE-1 in *GFP-Tg* mice, explicitly indicating that the neo-liver NPCs were derived from recipient tissues. This result further prompted us to investigate whether the NPCs originated from bone marrow (BM) or other tissues. To address this issue, we

replaced the BM of wild-type mice with BM of *GFP*-Tg mice by irradiation followed by BM transplant (GFP-BMT mice, the GFP chimerism in the peripheral blood was 80.1–96.8%) and used these mice for neo-liver generation using GFP⁺ hepatocytes (Fig. 3G).

Immunofluorescence analysis of the neo-livers in the GFP-BMT mice on days 70–120 revealed that F4/80⁺ and LYVE-1⁺ cells co-localized with GFP. The relative GFP⁺ areas to F4/80⁺ and LYVE-1⁺ areas were more than 80% and 50%, respectively. In marked contrast, none of the desmin⁺ cells showed GFP signals. These data suggested that a significant proportion of F4/80⁺ and LYVE-1⁺ cells in the neo-livers were of BM origin, whereas desmin⁺ cells were originated from non-BM tissues. These findings intrinsically suggested that hepatocytes, nestled healthfully at the ectopic site, recruited NPCs from recipient tissues including the BM and these NPCs were directed to be liver-specific phenotypic cells during the neo-liver morphogenetic processes.

In addition, we observed the emergence of bile duct cells in the neo-livers by the detection of CK19⁺/EpCAM⁺/Sox9⁺ cells in the vicinity of the venous branches extending from the renal parenchyma into the proximal region of the neo-liver at 1.5 yrs (Fig. 4A). These triple-positive cells were also observed in the neo-liver at 2.4 yrs. Although these triple-positive cells in the neo-livers did not form tubular structures, some of these cells were potentially mature bile duct cells as evidenced by the expression of cystic fibrosis transmembrane conductance regulator (CFTR), a molecule expressed by mature bile duct cells in the liver (Fig. 4B). It is also important to note that cholestatic hepatocyte injury was not observed in the organ-sized neo-livers of the MCT/PHx-treated mice (Fig. 2D, E), possibly indicating the functional secretion of bile acids from the neo-livers. In addition, we measured the serum bilirubin and bile acids levels and found no significant differences in each value between MCT/PHx-treated mice with and without neo-livers at day 270 (Table S2). These results suggested that the neo-liver created under the kidney capsule may have a mechanism that safely excretes bile out of the body (e.g., excretion of bile into urine).

Expression of liver regeneration-related genes in the neo-liver

Many cytokines and growth factors secreted from liver NPCs are implicated in the promotion of hepatocyte proliferation.^{2,3,19} Hepatocyte growth factor (*HGF*), interleukin (*IL*)-6, transforming growth factor- α (*TGF*- α), and tumor necrosis factor (*TNF*) are up-regulated during liver regeneration. To determine whether these genes are up-regulated during the enlargement process of the neo-livers, we determined the gene expression levels of *HGF*, *IL*-6, *TGF*- α , and *TNF* on days 250–300 by quantitative reverse transcription PCR (RT-qPCR). As a result, we found that ectopic neo-livers as well as the injured recipient livers showed increased levels of these genes compared with normal livers (Fig. 5A). In particular, expression of the *IL*-6 gene was markedly up-regulated (6.2 ± 3.1 -fold) in the neo-livers. The *IL*-6/STAT3 signaling pathway is important for mitogenesis and anti-apoptosis of hepatocytes during liver regeneration.^{20, 21} Therefore, we next examined whether the *IL*-6/STAT3 signaling pathway was activated in the neo-livers. Our histological observation revealed that phospho-STAT3 was found in the nuclei of hepatocytes in the neo-livers on days 30 and 150, but not in the normal livers or in the neo-livers in mice harboring intact native livers (Fig. 5B). These data suggested that the *IL*-6/STAT3 pathway was involved in the enlargement process of the neo-livers.

Structural and functional characterization of the neo-liver

Liver zonation is characterized by regional differences in the metabolic and enzymatic functions along the centrilobular/portal axis. Many genes and their protein products are expressed within the liver lobules in a zone-specific manner. In the normal livers, the expressions of E-cadherin, LYVE-1, and glutamine synthetase (GS) are restricted to the hepatocytes in zone 1 (peri-portal region), LSECs in zone 2 (intermediate region), and hepatocytes in zone 3 (peri-central region), respectively.^{22–24} In the neo-livers, at day 150, an E-cadherin-positive zone 1 locating in close proximity to the renal parenchyma, a LYVE-1-positive zone 2 locating between zones 1 and 3, and a GS-positive zone 3 locating around the vessels near the renal capsule were observed (Fig. 6A). Recently, researchers have elucidated that zone 3 hepatocytes express *Axin2* and *Tbx3*, which contribute to homeostatic hepatocyte renewal.²⁵ We therefore observed the expressions of *Axin2* and *Tbx3* mRNAs in the neo-livers, and found that they were specifically localized in the perivascular hepatocytes at 1.1 yrs (Fig. S4). An intraperitoneal inoculation with phenobarbital (an inducer of cytochrome P450 (CYP) 2B) in mice harboring a neo-liver was found to promote the robust expression of CYP2B in zone 3 hepatocytes within the neo-livers compared with the hepatocytes in other zones (Fig. S5). A RT-qPCR analysis (Fig. 6B) and microarray profiling (Fig. 6C) of liver-specific genes showed that the gene profiles within the neo-livers at days 250–300 were comparable to those measured in the normal and host livers but clearly different from the profiles of the host kidneys. Additionally, on day 245, we injected a hepatocyte-specific contrast agent, gadolinium ethoxybenzyl diethylenetriaminepentaacetic acid (Gd-EOB-DTPA, a functional marker of hepatocytes), into the general circulation of the recipient mice to perform magnetic resonance imaging (MRI).²⁶ As shown in Fig. S6A–F the T1-weighted and fat-saturated T1-weighted images showed a crescent-shaped region with enhanced contrast on the left kidney surface (Fig. S6G). We calculated the relative enhancement after the Gd-EOB-DTPA injection and found that both the host liver and the ectopic neo-liver tissues showed similar levels of relative enhancement in the first scan (Fig. S6H). These findings indicate that hepatocytes can form a complex 3D neo-liver at ectopic sites that is very similar to a normal liver in terms of function, gene expression profiling, and architecture, i.e., liver-specific vascular systems and zonal heterogeneity.

Therapeutic value of the neo-liver in lethal metabolic liver disease

We next assessed the therapeutic value of the neo-liver in *Fah*^{−/−} mice that suffer from lethal hepatic dysfunction. Specifically, these mice are used as a model of tyrosinemia type I. *Fah*-deficient tyrosinemic mice die shortly after the withdrawal of a therapeutic compound, 2-(2-nitro-4-trifluoro-methylbenzoyl)-1,3 cyclohexanedione (NTBC),⁹ and consequently are an ideal model to test the therapeutic efficacy of our neo-liver system. The neo-liver was engineered using *Fah*^{+/GFP} hepatocytes under the left kidney capsule space of *Fah*^{−/−} mice, followed by the subsequent withdrawal of NTBC. As a result, the neo-liver with *Fah*^{+/GFP} hepatocytes was also enlarged in the left kidney of *Fah*^{−/−} mice at 12 wks (Fig. 7A, B). The weight of the left kidney was approximately triple that of the right kidney at 24 wks (Fig. 7C). We observed dense neovascular networks in the neo-livers at 12 wks (Fig. 7D). All *Fah*^{−/−} mice with a neo-liver survived over a 20-week period even without NTBC (Fig. 7E). In marked contrast, all non-treated *Fah*^{−/−} mice died within 8 wks without the NTBC treatment.

To demonstrate that the neo-liver was responsible for the extended survival of the *Fah*^{-/-} mice, the left kidney harboring the neo-liver was excised at 22 wks. All nephrectomized mice perished within 7 days after this procedure, whereas the remaining non-nephrectomized mice continued to survive (Fig. 7E). These results clearly validated the significant life-supporting functions of the ectopic neo-liver in a mouse model of lethal hepatic failure.

In addition, we investigated whether NPCs emerged or not in the neo-livers of *Fah*^{-/-} mice at 4, 13, and 24 wks (Fig. 8). At 4 wks, a number of LYVE-1⁺ endothelial cells already existed between hepatocytes. In contrast, desmin⁺ and F4/80⁺ cells were hardly observed in the neo-liver at 4 wks. Thereafter, the densities of desmin⁺ and F4/80⁺ cells in the neo-liver were increased, and the ratios of these cells at 24 wks were comparable to those of the normal liver. From these findings, three types of NPCs were also proved to be recruited in the neo-liver of the *Fah*^{-/-} mice, as in the case of the MCT/PHx-treated mice.

Discussion

We previously reported that hepatocytes engrafted under the kidney capsule transiently (approximately for 2 wks) underwent proliferation after 70% hepatectomy.⁸ However, hepatocyte growth was terminated when the original mass of the native liver was recovered. In this study, we employed two mouse models with sustained and severe hepatocyte injury. In the MCT/PHx model, hepatocyte growth in the injured native liver was inhibited over 1 yr after PHx. The liver of *Fah*^{-/-} mice also exhibited continuous severe hepatocyte injury with necrosis and inflammation. The massive and continuous loss of hepatocytes of the native liver in these two liver injury models permitted the formation of the large-sized neo-liver containing liver-specific NPCs following an extensive and selective growth of engrafted hepatocytes under the kidney capsule.

One of the most prominent findings of our experiments was that the neo-liver NPCs were of recipient origin. The desmin⁺ HSC-like cells in the neo-livers (termed neo-liver HSCs) were derived from recipient tissues other than BM. It has been reported that liver mesothelial cells can transdifferentiate into HSCs in the injured liver.²⁷ The mesothelium tissue, derived from the embryonic mesoderm, covers internal organs including liver and kidney. Therefore, we speculate that kidney mesothelial cells might have transdifferentiated into the neo-liver HSCs.

In contrast, our investigation demonstrated that significant populations of F4/80⁺ cells (termed neo-liver KCs) and LYVE-1⁺ cells (termed neo-liver ECs) in the neo-livers originated from the BM. One of the interesting findings in regard to the neo-liver ECs was the formation of fenestrations on day 150 (Fig. 3E), which suggested that neo-liver ECs were mature and functional as in the case of LSECs in the native liver. These results are consistent with previous reports demonstrating that BM cells are the major cell source for the LSEC repopulation in the native liver after liver injury. In recent reports, the BM-derived cells, characterized as CD133⁺45⁺31⁺ cells, were identified as progenitor cells for LSECs (BM SPCs).²⁸ BM SPCs were found to be recruited into the liver under the guidance of vascular endothelial growth factor (VEGF) that was produced by the liver, followed by their

differentiation into mature LSECs during liver injury.²⁹ The occupancy ratio of BM SPCs-derived LSECs in the liver gradually increased during the liver regeneration process.³⁰ It is of great importance to note that the LSECs derived from BM SPCs also have fenestrations in the sieve plates, and these fenestrations are essential for hepatocytes to exert liver-specific functions including metabolism, protein secretion, and detoxification.

There has been a great controversy regarding the question whether tissue-resident macrophages including liver KCs are derived from BM-derived monocytes or self-renewing embryo-derived tissue-resident macrophages.³¹ In the most prevalent recent theory, the KCs are originated from the embryonic yolk sac or fetal liver and self-renew with minimal contribution of monocytes in the steady state.³² Meanwhile, monocyte-derived macrophages have been reported to differentiate into self-renewing KCs, when KCs are fully depleted in native liver.³³ Our study revealed that a large proportion of the neo-liver KCs were originated from BM when ectopic neo-livers were created using adult hepatocytes. Because KCs were absent in the neo-liver at the initial stage, differentiation of monocytes into KCs could have been promoted during the liver-organogenesis processes.

Aside from the origin of neo-liver NPCs, our data provided important evidence that liver organogenesis accompanying NPC recruitment could be reproduced around the engrafted hepatocytes in the kidney, even though the subrenal space at the stage of hepatocyte transplantation did not possess liver-specific conditions such as the presence of liver NPCs, the portal bloodstream, and innervation. We consider that engrafted hepatocytes induced the migration and differentiation of NPCs by providing appropriate housing through the formation of small 3D tissues consisting of hepatocytes and secretion of cytokines and growth factors from hepatocytes in response to native liver injury.

It is known that various growth factors are deeply involved in the regeneration process of the native liver. For example, liver NPCs produce growth factors and cytokines such as IL-6, HGF, and TNF and promote liver regeneration. BM-derived LSECs have been reported to produce HGF at higher levels than pre-existing LSECs in the injured liver.³⁴ In the present study, we confirmed that the mRNA expression levels of these genes (*HGF*, *IL-6*, and *TGF- α*) at days 250–300 in the neo-livers were higher than those in the normal livers. These results underscore that the neo-liver possesses adequate functionality to express these factors promoting its enlargement in response to the stimuli arising from the chronic native liver injury.

The created neo-livers showed structural and functional similarities with the native livers. First, the formation of metabolic liver zonation (zones 1, 2, and 3) was observed on day 150. Liver zonation is thought to be regulated by the gradients of signaling molecules such as oxygen, hormones, cytokines, nutrients, and metabolites along the periportal-to-perivenous blood flow.³⁵ In addition, the Wnt/ β -catenin pathway plays a key role in the maintenance of liver zonation and the regional gene activation. The Wnt signals secreted from liver KCs are required to maintain the liver zonation during liver regeneration.³⁶ In light of these findings, it could be assumed that the gradient of signaling molecules was reproduced throughout the microcirculation within the neo-livers, and the Wnt signals secreted from neo-liver KCs were properly delivered to hepatocytes, and that both these phenomena contributed to the

reproduction of the proper liver zonation. Second, we confirmed that the pericentral hepatocytes expressed *Axin2* and *Tbx3* in the neo-livers. *Axin2*- and *Tbx3*-positive pericentral hepatocytes are known to contribute to the homeostasis of the liver under normal conditions.²⁵ The liver-specific niche of pericentral cells is also maintained by Wnt signals secreted from LSECs residing near the central vein. These results strongly implied that hepatocytes possess the ability to reorganize the microenvironments to be suitable for hepatocytes themselves, in terms of the pericentral niche of *Axin2*- and *Tbx3*-positive hepatocytes, via the recruitment and differentiation of neo-liver ECs.

In summary, we clearly demonstrated that a small number of engrafted adult hepatocytes at an ectopic site played central roles in liver morphogenesis through NPC recruitment, and these hepatocytes demonstrated an amazing ability to form a whole, complex organ-sized neo-liver having the architecture and functions of a native liver. Our findings clarified the significant roles of adult hepatocytes in neo-liver construction; adult hepatocytes should thus prove to be extremely useful not only for creating new liver systems themselves, but also for elucidating the molecular mechanisms underlying dynamic regeneration behavior and homeostasis maintenance of the liver. In addition, organ engineering using hepatocytes at extrahepatic sites has great therapeutic potential and medical import for patients with liver diseases accompanied by severe hepatocyte loss in the native liver such as tyrosinaemia type I, α -1 antitrypsin deficiency, and argininosuccinate lyase deficiency, a certain form of urea cycle disorder.

Supplementary Material

Refer to Web version on PubMed Central for supplementary material.

Acknowledgments

We would like to thank Dr. T. Tsuji (Bayer Diagnostics Japan) for assisting with the MR imaging, Dr. A. Miyajima (University of Tokyo) for providing the stabilin-2 antibody, Dr. G. L. Bumgardner for providing the hA1AT-FVB/N mouse line, Ms. M. Yoshimura, Ms. K. Kawahara, and Ms. K. Kanegae for their technical assistance, and Dr. F. Park (Medical College of Wisconsin) for his editorial assistance on this manuscript.

Financial Support: This work was supported in part by the Creation of Innovation Centers for Advanced Interdisciplinary Research Areas Program in the Project for Developing Innovation Systems (K.O., T.O.) from the Ministry of Education, Culture, Sports, Science, and Technology (MEXT) of Japan, JSPS KAKENHI Grant Numbers 26670587 (K.O.), 16K01355 (K.O.), 26350530 (R.U.), and 16J40041 (R.U.), a Health and Labour Sciences Research Grant for Research on HIV/AIDS (A.Y.) from the Ministry of Health, Labour and Welfare (MHLW) of Japan, and NIH grant R01 DK085711 (E.L.).

References

1. Overturf K, al-Dhalimy M, Ou CN, Finegold M, Grompe M. Serial transplantation reveals the stem-cell-like regenerative potential of adult mouse hepatocytes. *Am J Pathol.* 1997; 151:1273–1280. [PubMed: 9358753]
2. Taub R. Liver regeneration: from myth to mechanism. *Nat Rev Mol Cell Biol.* 2004; 5:836–847. [PubMed: 15459664]
3. Michalopoulos GK. Liver regeneration. *J Cell Physiol.* 2007; 213:286–300. [PubMed: 17559071]
4. Sandgren EP, Palmiter RD, Heckel JL, Daugherty CC, Brinster RL, Degen JL. Complete hepatic regeneration after somatic deletion of an albumin-plasminogen activator transgene. *Cell.* 1991; 66:245–256. [PubMed: 1713128]

5. Overturf K, Al-Dhalimy M, Tanguay R, Brantly M, Ou CN, Finegold M, et al. Hepatocytes corrected by gene therapy are selected in vivo in a murine model of hereditary tyrosinaemia type I. *Nat Genet.* 1996; 12:266–273. [PubMed: 8589717]
6. Tatenos C, Yoshizane Y, Saito N, Kataoka M, Utoh R, Yamasaki C, et al. Near completely humanized liver in mice shows human-type metabolic responses to drugs. *Am J Pathol.* 2004; 165:901–912. [PubMed: 15331414]
7. Makowka L, Lee G, Cobourn CS, Farber E, Falk JA, Falk RE. Allogeneic hepatocyte transplantation in the rat spleen under cyclosporine immunosuppression. *Transplantation.* 1986; 42:537–541. [PubMed: 3538539]
8. Ohashi K, Waugh JM, Dake MD, Yokoyama T, Kuge H, Nakajima Y, et al. Liver tissue engineering at extrahepatic sites in mice as a potential new therapy for genetic liver diseases. *Hepatology.* 2005; 41:132–140. [PubMed: 15619229]
9. Komori J, Boone L, DeWard A, Hoppo T, Lagasse E. The mouse lymph node as an ectopic transplantation site for multiple tissues. *Nat Biotechnol.* 2012; 30:976–983. [PubMed: 23000933]
10. Bhatia SN, Underhill GH, Zaret KS, Fox IJ. Cell and tissue engineering for liver disease. *Sci Transl Med.* 2014; 6:245sr242.
11. Ohashi K, Yokoyama T, Yamato M, Kuge H, Kanehiro H, Tsutsumi M, et al. Engineering functional two- and three-dimensional liver systems in vivo using hepatic tissue sheets. *Nat Med.* 2007; 13:880–885. [PubMed: 17572687]
12. Witek RP, Fisher SH, Petersen BE. Monocrotaline, an alternative to retrorsine-based hepatocyte transplantation in rodents. *Cell Transplant.* 2005; 14:41–47. [PubMed: 15789661]
13. Friedman SL. Hepatic stellate cells: protean, multifunctional, and enigmatic cells of the liver. *Physiol Rev.* 2008; 88:125–172. [PubMed: 18195085]
14. Hume DA, Perry VH, Gordon S. The mononuclear phagocyte system of the mouse defined by immunohistochemical localisation of antigen F4/80: macrophages associated with epithelia. *Anat Rec.* 1984; 210:503–512. [PubMed: 6524692]
15. Nonaka H, Tanaka M, Suzuki K, Miyajima A. Development of murine hepatic sinusoidal endothelial cells characterized by the expression of hyaluronan receptors. *Dev Dyn.* 2007; 236:2258–2267. [PubMed: 17626278]
16. DeLeve LD. Liver sinusoidal endothelial cells in hepatic fibrosis. *Hepatology.* 2015; 61:1740–1746. [PubMed: 25131509]
17. Nakamura-Ishizu A, Morikawa S, Shimizu K, Ezaki T. Characterization of sinusoidal endothelial cells of the liver and bone marrow using an intravital lectin injection method. *J Mol Histol.* 2008; 39:471–479. [PubMed: 18751902]
18. Crawford JM, Mockel GM, Crawford AR, Hagen SJ, Hatch VC, Barnes S, et al. Imaging biliary lipid secretion in the rat: ultrastructural evidence for vesiculation of the hepatocyte canalicular membrane. *J Lipid Res.* 1995; 36:2147–2163. [PubMed: 8576641]
19. Fausto N. Liver regeneration. *J Hepatol.* 2000; 32:19–31.
20. Cressman DE, Greenbaum LE, DeAngelis RA, Ciliberto G, Furth EE, Poli V, et al. Liver failure and defective hepatocyte regeneration in interleukin-6-deficient mice. *Science.* 1996; 274:1379–1383. [PubMed: 8910279]
21. Taub R. Hepatoprotection via the IL-6/Stat3 pathway. *J Clin Invest.* 2003; 112:978–980. [PubMed: 14523032]
22. Kuo CF, Paulson KE, Darnell JE Jr. Positional and developmental regulation of glutamine synthetase expression in mouse liver. *Mol Cell Biol.* 1988; 8:4966–4971. [PubMed: 2905422]
23. Mouta Carreira C, Nasser SM, di Tomaso E, Padera TP, Boucher Y, Tomarev SI, et al. LYVE-1 is not restricted to the lymph vessels: expression in normal liver blood sinusoids and down-regulation in human liver cancer and cirrhosis. *Cancer Res.* 2001; 61:8079–8084. [PubMed: 11719431]
24. Doi Y, Tamura S, Nammo T, Fukui K, Kiso S, Nagafuchi A. Development of complementary expression patterns of E- and N-cadherin in the mouse liver. *Hepatol Res.* 2007; 37:230–237. [PubMed: 17362306]
25. Wang B, Zhao L, Fish M, Logan CY, Nusse R. Self-renewing diploid Axin2⁺ cells fuel homeostatic renewal of the liver. *Nature.* 2015; 524:180–185. [PubMed: 26245375]

26. Weinmann HJ, Schuhmann-Giampieri G, Schmitt-Willich H, Vogler H, Frenzel T, Gries H. A new lipophilic gadolinium chelate as a tissue-specific contrast medium for MRI. *Magn Reson Med*. 1991; 22:233–237. [PubMed: 1812351]
27. Li Y, Wang J, Asahina K. Mesothelial cells give rise to hepatic stellate cells and myofibroblasts via mesothelial-mesenchymal transition in liver injury. *Proc Natl Acad Sci U S A*. 2013; 110:2324–2329. [PubMed: 23345421]
28. Harb R, Xie G, Lutzko C, Guo Y, Wang X, Hill CK, et al. Bone marrow progenitor cells repair rat hepatic sinusoidal endothelial cells after liver injury. *Gastroenterology*. 2009; 137:704–712. [PubMed: 19447108]
29. DeLeve LD. Liver sinusoidal endothelial cells and liver regeneration. *J Clin Invest*. 2013; 123:1861–1866. [PubMed: 23635783]
30. Wang L, Wang X, Wang L, Chiu JD, van de Ven G, Gaarde WA, et al. Hepatic vascular endothelial growth factor regulates recruitment of rat liver sinusoidal endothelial cell progenitor cells. *Gastroenterology*. 2012; 143:1555–1563. e1552. [PubMed: 22902870]
31. Davies LC, Jenkins SJ, Allen JE, Taylor PR. Tissue-resident macrophages. *Nat Immunol*. 2013; 14:986–995. [PubMed: 24048120]
32. Krenkel O, Tacke F. Liver macrophages in tissue homeostasis and disease. *Nat Rev Immunol*. 2017; 17:306–321. [PubMed: 28317925]
33. Scott CL, Zheng F, De Baetselier P, Martens L, Saeys Y, De Prijck S, et al. Bone marrow-derived monocytes give rise to self-renewing and fully differentiated Kupffer cells. *Nat Commun*. 2016; 7:10321. [PubMed: 26813785]
34. Wang L, Wang X, Xie G, Wang L, Hill CK, DeLeve LD. Liver sinusoidal endothelial cell progenitor cells promote liver regeneration in rats. *J Clin Invest*. 2012; 122:1567–1573. [PubMed: 22406533]
35. Jungermann K, Kietzmann T. Oxygen: modulator of metabolic zonation and disease of the liver. *Hepatology*. 2000; 31:255–260. [PubMed: 10655244]
36. Yang J, Mowry LE, Nejak-Bowen KN, Okabe H, Diegel CR, Lang RA, et al. beta-catenin signaling in murine liver zonation and regeneration: a Wnt-Wnt situation. *Hepatology*. 2014; 60:964–976. [PubMed: 24700412]

Lay summary

The role of adult hepatocytes at ectopic locations has not been clarified. In this study, we demonstrated that engrafted hepatocytes in the kidney proliferated, recruited NPCs from host tissues including BM, and finally created an organ-sized, complex liver system that exhibited liver-specific architectures and functions. Our results revealed previously undescribed functions of hepatocytes to direct liver organogenesis through non-parenchymal cell recruitment and organize multiple cell types into a complex 3D liver at ectopic sites.

Highlights

- Hepatocytes engrafted in the kidney created an organ-sized and complex liver.
- At least three types of liver-specific NPCs were recruited in the neo-liver.
- Recruited NPCs were originated from the host tissues including bone marrow.
- The neo-liver in the kidney exhibited liver-specific functions and architectures.

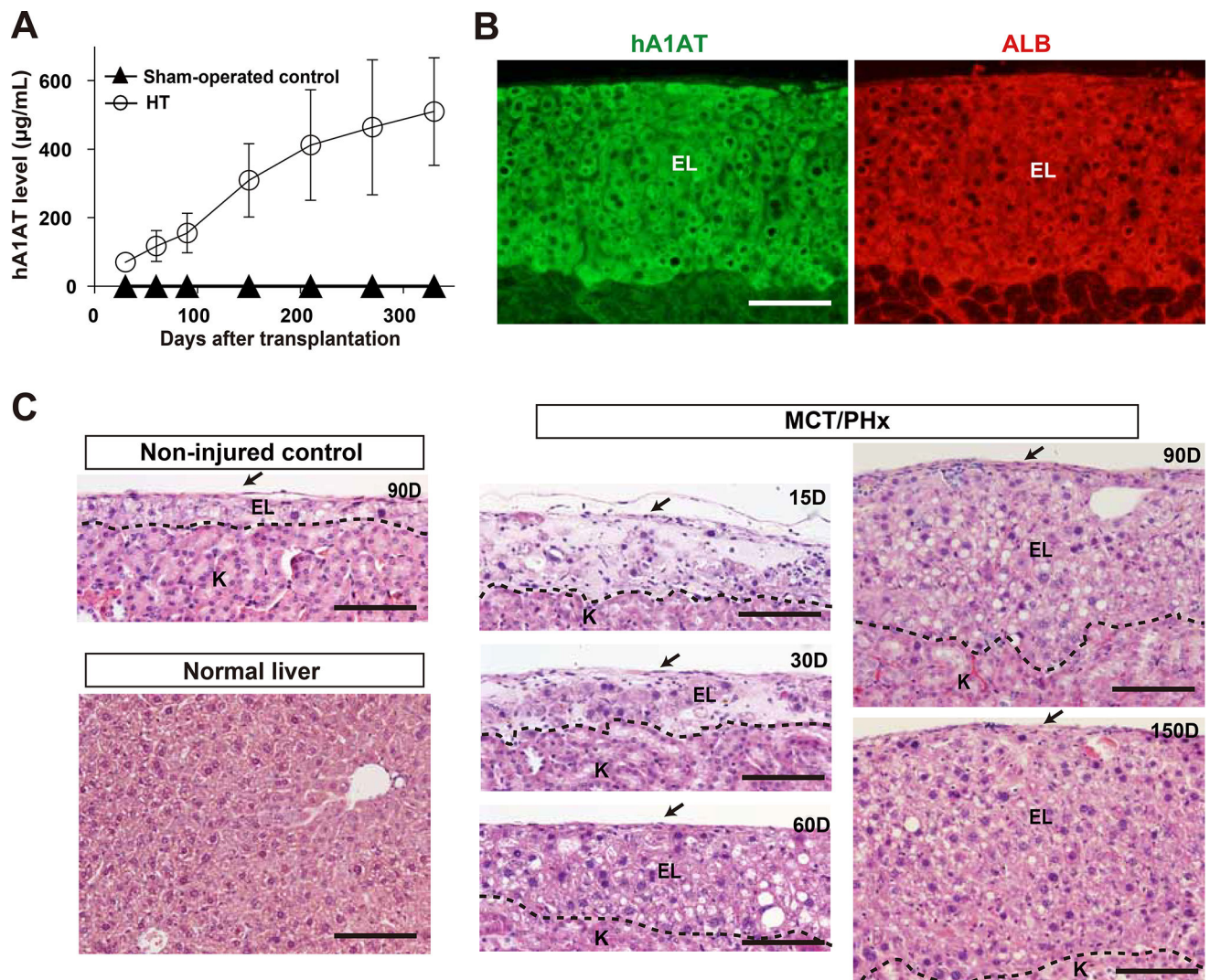


Fig. 1. Formation of an ectopic neo-liver under the kidney capsule

(A) The serum hA1AT concentration was measured with (HT; circle, $n = 18$) or without (sham-operated control; triangle, $n = 8$) hepatocyte transplantation in mice harboring MCT/PHx-induced injured livers. Mean \pm SD values are shown. (B) Immunohistochemistry for hA1AT and mouse albumin (ALB) of a neo-liver in recipient mice with native liver injury on day 90. (C) H&E staining of the neo-livers in mice with or without native liver injury and of the normal liver. EL: ectopic neo-liver; K: kidney parenchyma. Arrows = kidney capsule; dotted lines = boundary between the neo-liver and the kidney parenchyma. Scale bars: 100 µm in B and C.

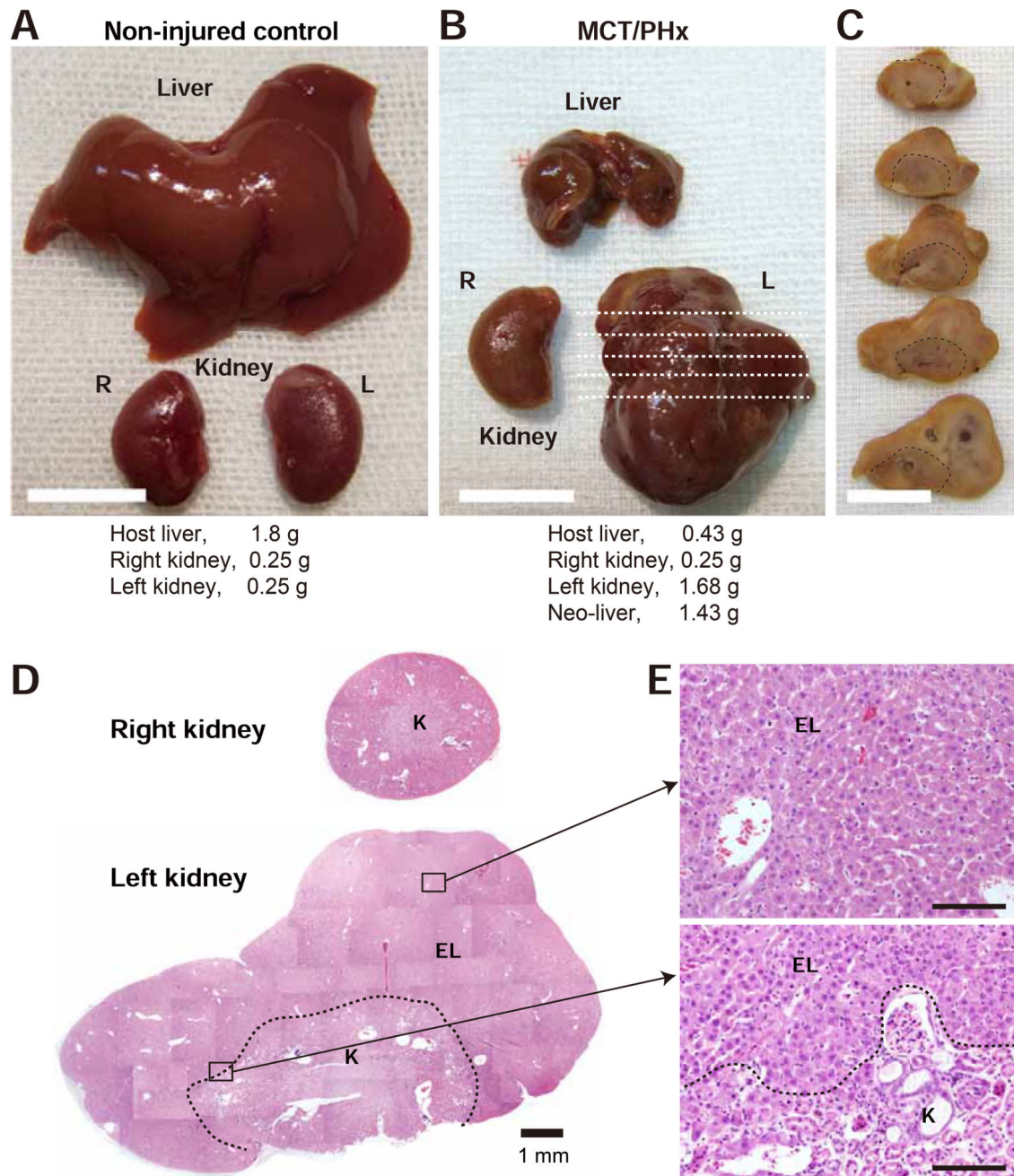


Fig. 2. Formation of an organ-sized liver in the kidney of mice harboring MCT/PHx-induced injured livers

(A,B) The gross appearance of the host native liver and the right and left kidneys of non-injured control mice (A) and mice with an ectopic neo-liver in the left kidney that were followed for 2.4 yrs (B). (C) Sequential segments as indicated by the white dashed lines in B were excised from the left kidney with the neo-liver. (D) H&E staining of the right and left kidneys in B. (E) The histological appearances of the areas indicated by the rectangular regions in D are shown at a higher magnification. EL: ectopic neo-liver; K: kidney parenchyma. Arrows = kidney capsule; dotted lines = boundary between the neo-liver and the kidney parenchyma. Scale bars: 1 cm in A–C, 1 mm in D, and 100 μ m in E.

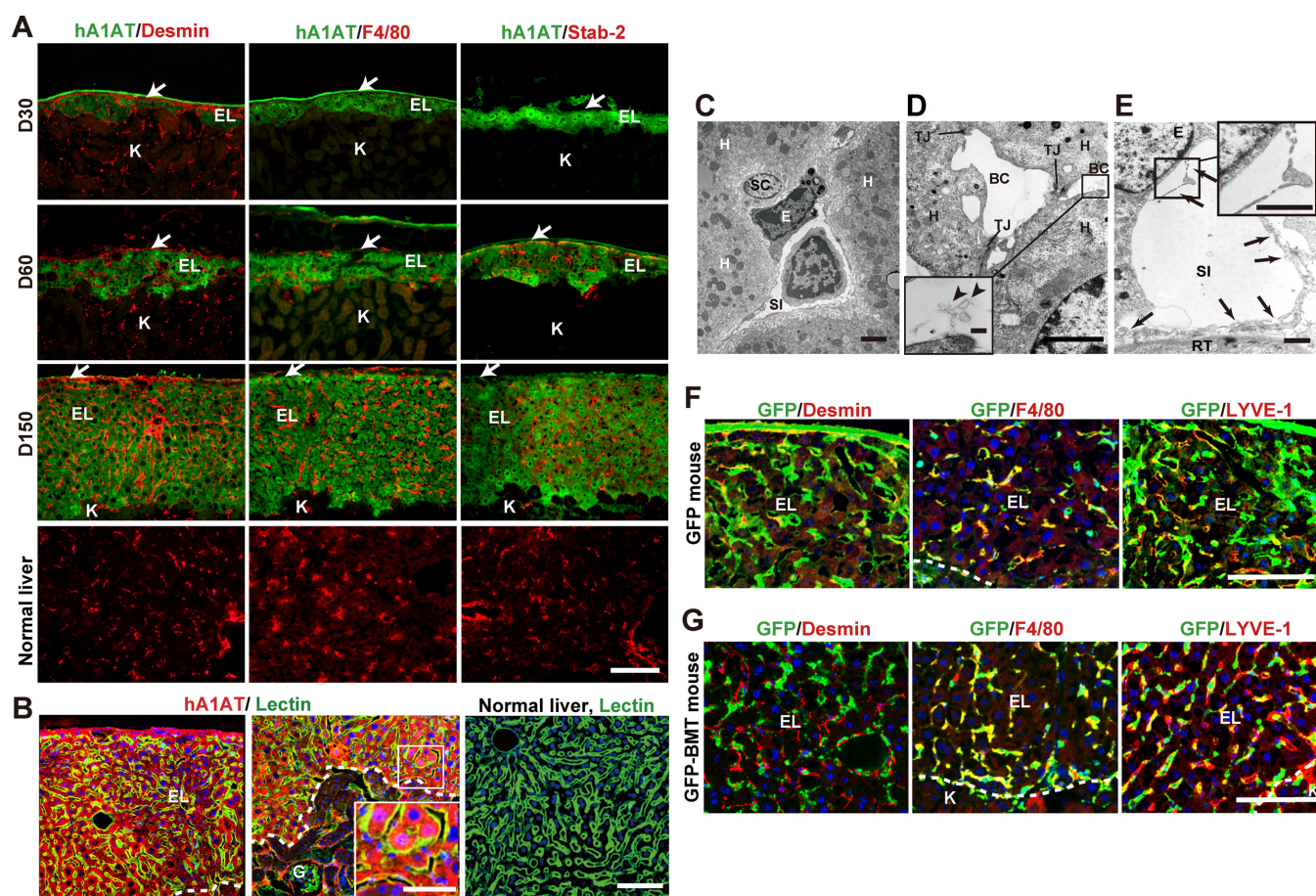


Fig. 3. Organogenesis of the liver with liver-specific non-parenchymal cells under the kidney capsule

(A) Immunostaining with hA1AT (*green*) and with desmin, F4/80, or stabilin-2 (*red*) was performed in the normal liver and neo-livers. (B) Distribution of the endothelial cells as determined by the FITC-labeled tomato lectin-binding pattern in the ectopic liver on day 180 and in the normal liver. (C–E) Transmission electron microscope images of the neo-liver on day 150. (F,G) Confocal images for GFP (*green*) and desmin (*red*), F4/80 (*red*), or LYVE-1 (*red*) on days 70–120. GFP[−] hepatocytes were transplanted into MCT/PHx-treated GFP transgenic (F) or GFP⁺-bone marrow transplanted (BMT) wild-type mice (G). EL: ectopic neo-liver; K: kidney parenchyma; H: hepatocyte; E: endothelial cell; SI: sinusoid; RT: renal tubule; BC: bile canaliculus; SC: stellate cell; TJ: tight junction. White arrowheads = kidney capsule; black arrows = fenestration of endothelial cells; black arrowheads = unilamellar lipid vesicles in the BC; dotted lines = boundary between the neo-liver and the kidney parenchyma. Scale bars: 100 μ m in A, B, F, and G, 50 μ m in the rectangular region in B, 2 μ m in C and D, 1 μ m in E, and 100 nm in the rectangular region in E.

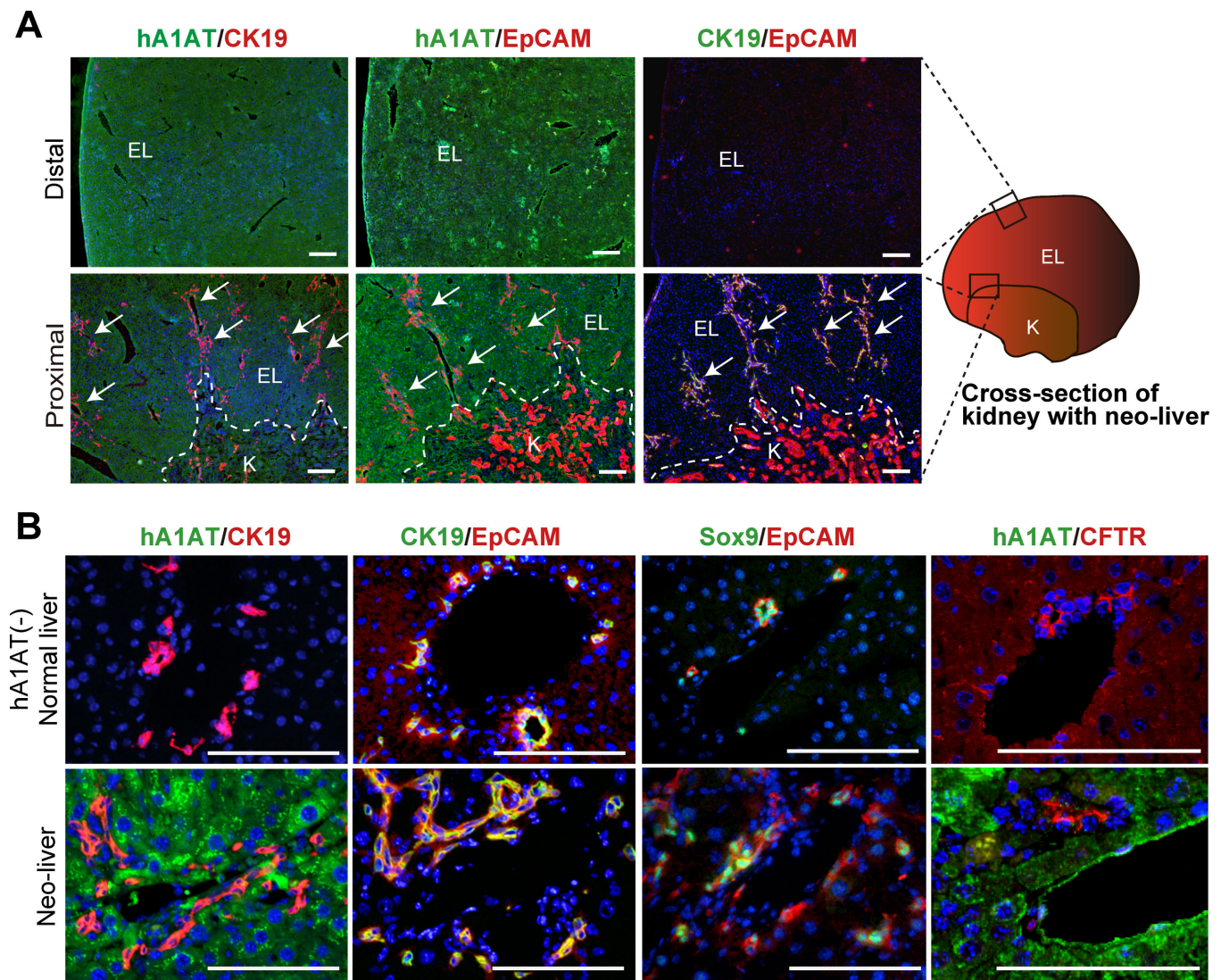


Fig. 4. Immunofluorescence staining for bile duct markers in the neo-liver

Immunostaining of the sections of the kidneys with the neo-liver created from hA1AT⁺ hepatocytes in the MCT/PHx-treated mice at 1.5 or 2.4 yrs after transplantation. (A) Low magnification images for the distal and proximal regions of the neo-liver. (B) High magnification images for the normal liver and the neo-liver. Immunohistochemical localizations of cytokeratin 19 (CK19, *green* or *red*), epithelial cell adhesion molecule (EpCAM, *red*), and Sox9 (*green*) at 1.5 yrs (A,B) and cystic fibrosis transmembrane conductance regulator (CFTR, *red*) at 2.4 yrs (B) were examined. Sections were counterstained with DAPI in blue. Arrows denote CK19 and EpCAM positive cells in the neo-liver. Dotted lines = boundary between the neo-liver and the kidney parenchyma. EL: ectopic neo-liver, K: kidney parenchyma. Scale bars: 200 μm in A, 100 μm in B.

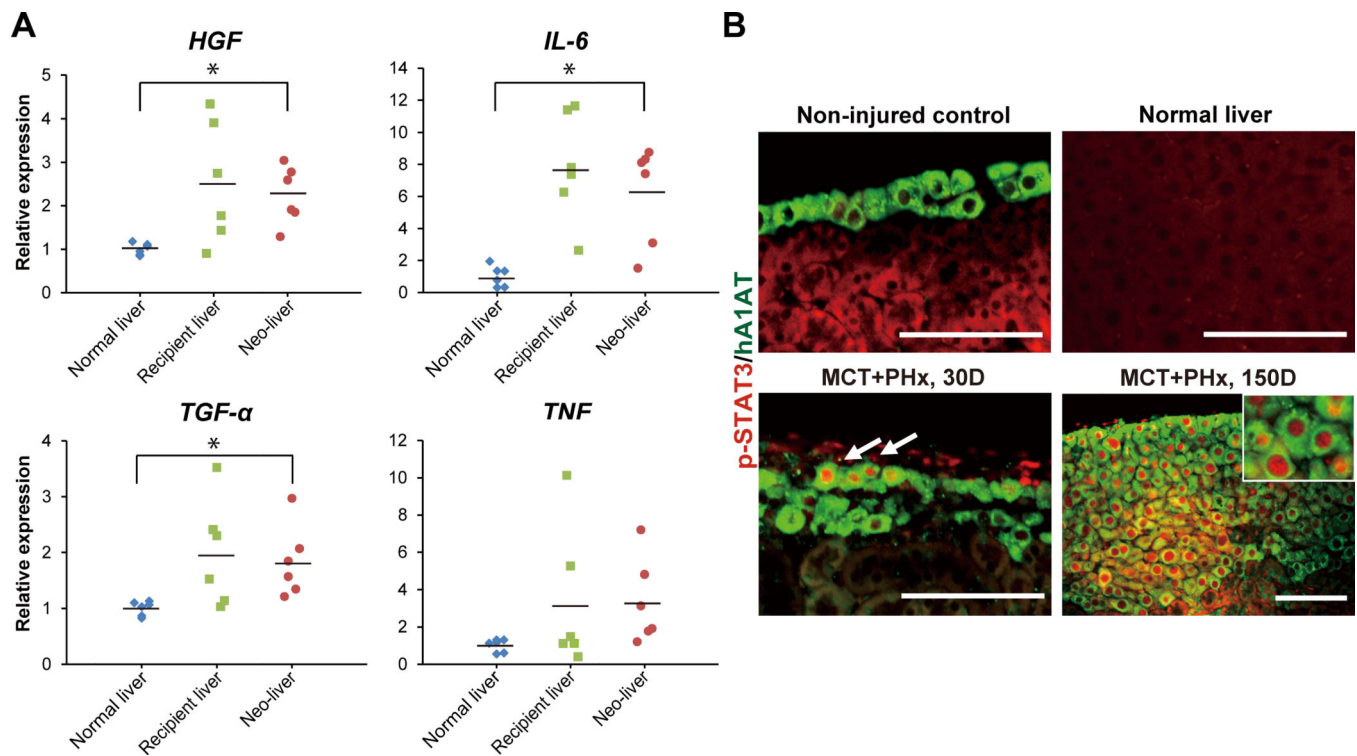


Fig. 5. Expression of liver regeneration-related growth factors and cytokines during neo-liver enlargement

(A) Gene expression analysis of *HGF*, *IL-6*, *TGF-α*, and *TNF* in the normal livers of non-injured control mice, recipient injured livers and neo-livers of mice harboring MCT/PHx-induced injured livers on days 250–300 by RT-qPCR. The values are the calculated fold changes relative to the expression levels of the normal liver ($n = 6$). The gene expression levels normalized to the *RPL4* expression levels. * $P < 0.05$ versus the normal liver, one way ANOVA with Tukey's or Games-Howell post-hoc analysis. (B) Immunohistochemistry for hA1AT (green) and phospho-STAT3 (p-STAT3, red) of the neo-livers in mice with (days 30 and 150) or without (day 150) liver injury and of the normal liver. Arrows denote p-STAT3 positive cells. Scale bars: 100 μm .

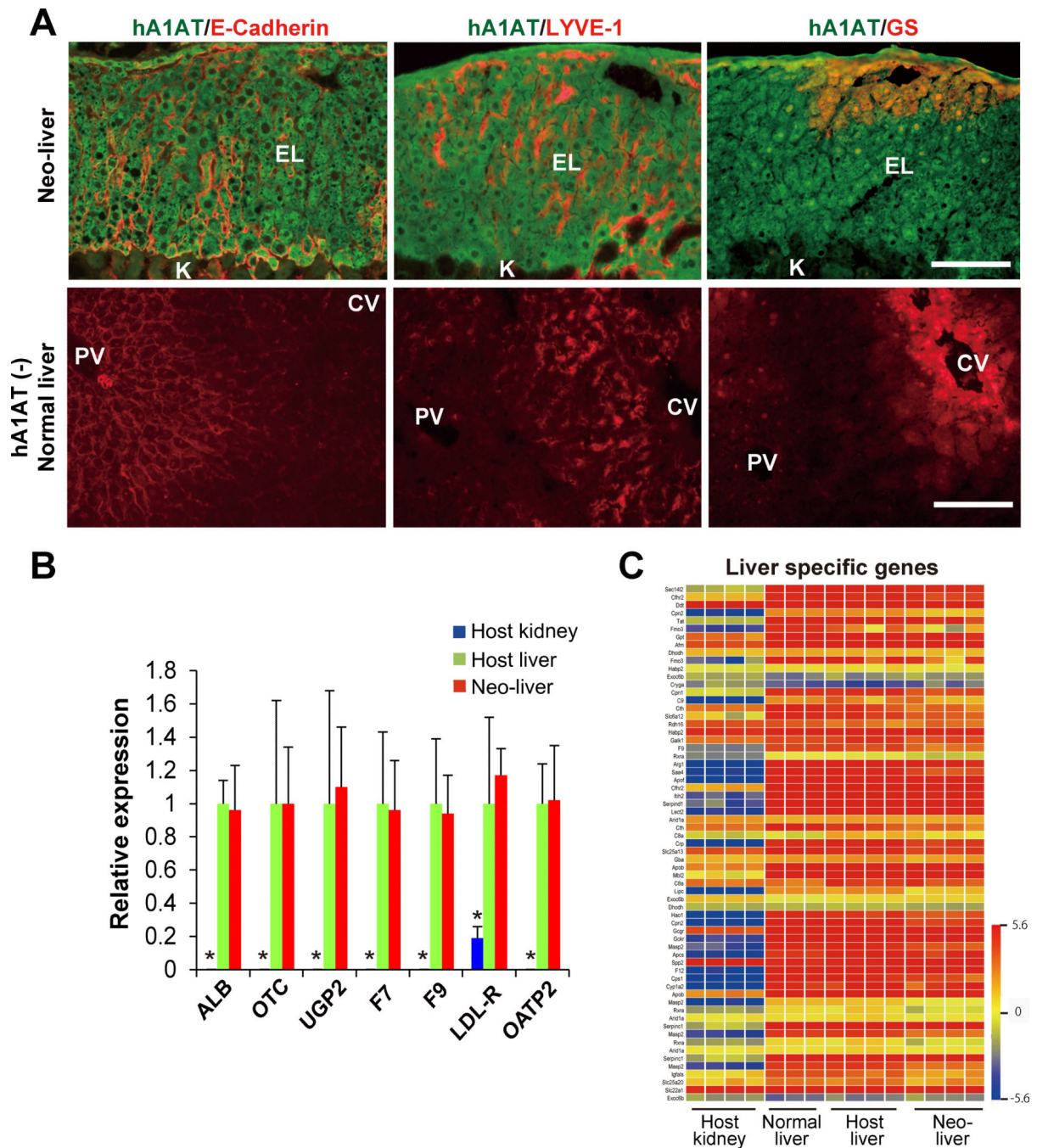


Fig. 6. Formation of a functional neo-liver with liver-specific zones and gene expressions
(A) Immunostaining for hA1AT (*green*) and E-cadherin, LYVE-1, or glutamine synthetase (GS) (*red*) in the neo-livers composed of hA1AT⁺ hepatocytes in MCT/PHx-treated mice at day 150 and in the normal livers of wild-type mice. (B) Gene expression analysis of the host kidneys, host livers, and neo-livers on days 250–300 by RT-qPCR. The values are the calculated fold changes relative to the expression levels of the host liver; mean \pm SD values are shown (n = 6). The gene expression levels normalized to the *RPL4* expression levels. **P* < 0.05 versus the host liver, one way ANOVA with Tukey's post-hoc analysis. (C) Heatmap

of 58 liver-specific genes in a large-scale microarray analysis (n =3 or 4). EL: ectopic neo-liver; K: kidney parenchyma; PV: portal vein; CV: central vein. Scale bar: 100 μ m in A.

Author Manuscript

Author Manuscript

Author Manuscript

Author Manuscript

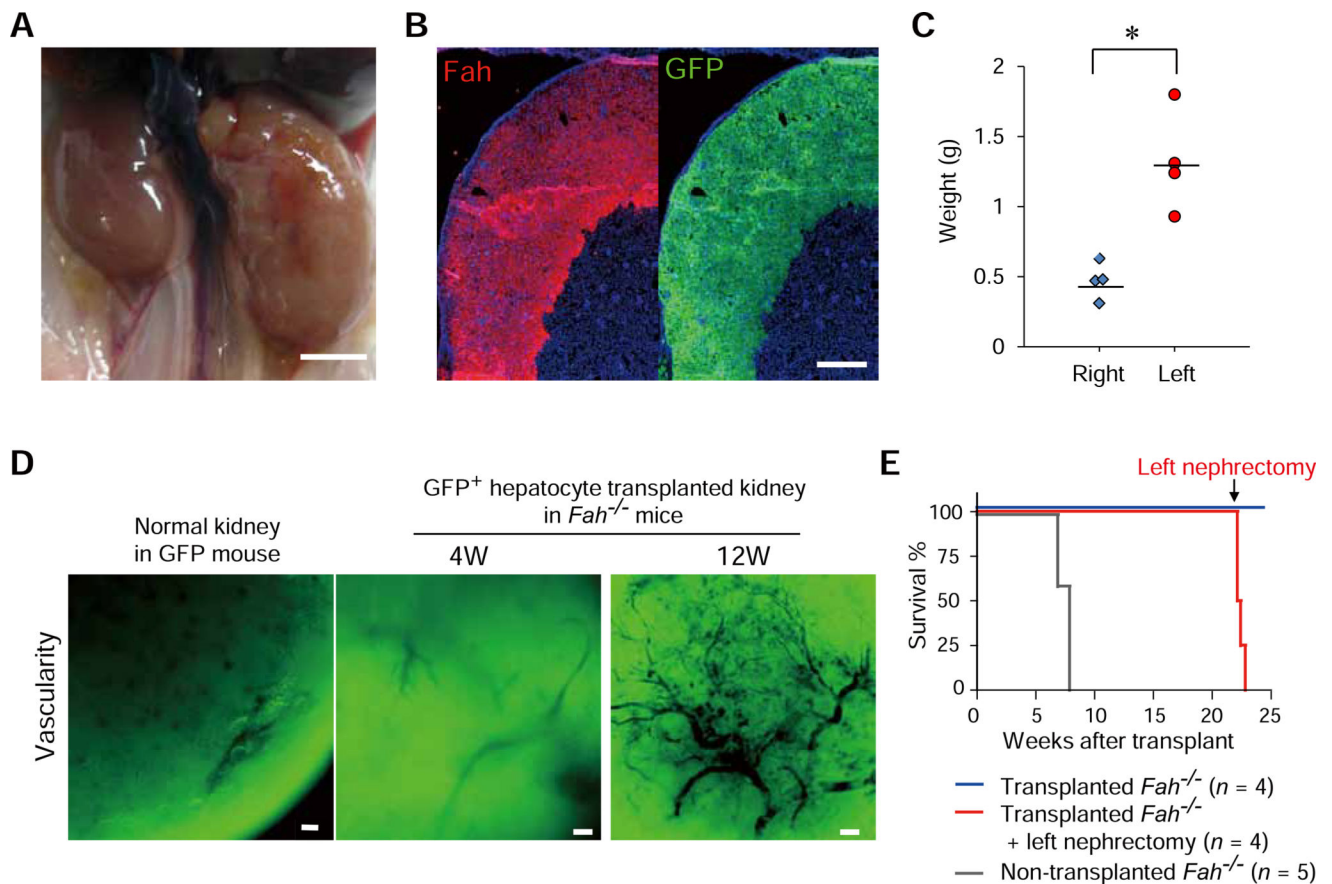


Fig. 7. Life-supporting effects of the neo-livers in *Fah*-deficient mice with lethal hepatic failure
 Neo-livers were engineered under the left kidney capsule of *Fah*^{-/-} mice using *Fah*⁺/GFP⁺ hepatocytes. (A) Macroscopic image of *Fah*^{-/-} mouse kidneys with (right) or without (left) neo-liver formation after 12 wks following the hepatocyte transplantation. (A) Immunofluorescence of *Fah* (red) and GFP (green) of the neo-liver at 12 wks. (C) Weights of the right and left kidneys at 24 wks (n = 4). *P < 0.05 versus the right kidney, student's *t*-test. (D) Vascularization of the neo-liver composed of GFP⁺ hepatocytes. Whole-mount images of fluorescence microscopy at 4 and 12 wks and compared with a normal kidney from a GFP transgenic mouse. Blood vessels are shown in black (GFP⁻). (E) Kaplan-Meier survival curves of the *Fah*^{-/-} mice with (blue and red) and without the neo-liver (black). At 22 wks, a nephrectomy of the left kidney with the neo-liver was performed in 4 mice (red). Scale bars: 5 mm in A, 500 μm in B, and 100 μm in D.

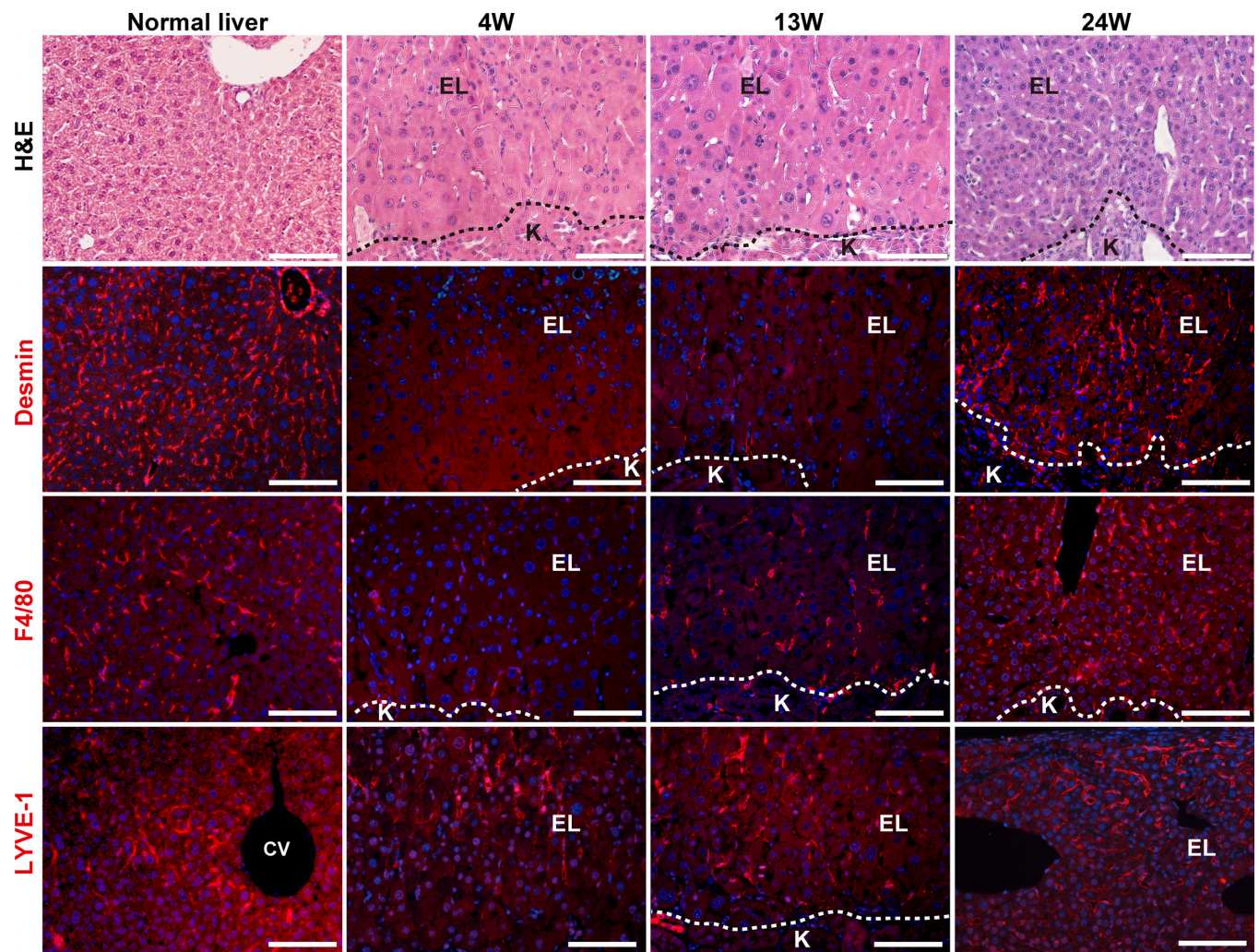


Fig. 8. Recruitment of NPCs in the neo-liver under the kidney capsule of *Fah*-deficient mice
H&E staining and immunohistochemistry for desmin, F4/80, or LYVE-1 (*red*) in the normal liver of a wild-type mouse and in the neo-livers under the kidney capsule of *Fah*^{-/-} mice at 4, 13, and 24 wks after transplantation. For immunofluorescence staining, sections were counterstained with DAPI in blue. Dotted lines = boundary between the neo-liver and the kidney parenchyma. EL: ectopic neo-liver; K: kidney parenchyma; CV: central vein. Scale bars: 100 μm.